Iterative Joint Detection, Decoding, and Synchronization with a Focus on Frame Timing

Daniel Jakubisin, Christopher Ian Phelps, and R. Michael Buehrer
Mobile and Portable Radio Research Group (MPRG), Wireless@VT,
Virginia Tech, Blacksburg, Virginia, USA. E-mail: {djj,chphelp2,buehrer}@vt.edu

***Abstract*—The concept of an iterative receiver has gained attention as a means of performing reliable synchronization, especially at the low signal-to-noise ratios enabled by error correction codes. In this paper, we consider joint detection of the information bits and estimation of the channel gain, carrier phase, symbol timing, frame timing, and noise power. Our particular focus is on the frame timing where we evaluate the complexity of the iterative receiver by characterizing the frame offset distribution. A method for dynamically choosing the set of frame offsets processed by the iterative receiver is presented. The receiver utilizes the expectation-maximization algorithm to perform estimation and the sum-product algorithm to perform soft demodulation and decoding. Numerical results are presented to characterize the frame offset distribution and to demonstrate the receiver's performance.**

I. Introduction

Following the success of iterative (turbo) decoding of channel codes, iterative algorithms have been developed for the purpose of *code-aided* or *turbo* synchronization or, more generally, incorporating synchronization into an *iterative receiver*. These iterative algorithms seek to approximate maximum likelihood (ML) or maximum *a posteriori* (MAP) joint detection of the information bits and estimation of the synchronization parameters. In general, the receiver may be responsible for estimation of the channel gain, carrier phase, symbol timing, frame timing, noise power, and more. Traditionally, in packet based systems, a known preamble enables reliable synchronization through data-aided methods. In contrast, the structure inherent in the channel code can be exploited within the context of the iterative receiver to perform reliable synchronization without a preamble.

The work of Noels *et al.* in [1] and [2] provides a theoretical framework for an iterative receiver for synchronization based on the expectation-maximization (EM) algorithm. Frequency, symbol timing, phase, and amplitude estimation are considered in the theoretical development of [1] and [2]. However, simulations are limited to phase estimation in [1] and joint frequency and phase estimation in [2]. The application of the EM algorithm to symbol timing synchronization is considered in [3] and [4].

The channel time delay may, in general, be greater than one symbol period and the rotational symmetry which exists in common phase-amplitude constellations will lead to an ambiguity in the phase offset. In order to handle this, the time offset is divided into a frame offset (integer multiples of the symbol period) and symbol timing offset (within the symbol period) and the phase offset is divided into a phase ambiguity (integer multiples of the rotational ambiguity in the constellation) and a continuous phase offset (within the ambiguity). Determining the frame offset and phase ambiguity becomes a detection problem which does not immediately fit into the EM algorithm's framework. Frame timing and phase ambiguity are approached from a hypothesis testing perspective in [5] where one of the presented methods is analogous to the EM algorithm and is given a more rigorous mathematical explanation in [6].

Unlike estimation of the other parameters, non-data-aided detection of the frame timing and phase ambiguity do not have the advantage of improving with the sequence length. In fact, without any knowledge of the data[1], detection of the phase ambiguity is not possible and detection of the frame timing (for example, using energy detection) is unreliable even at moderate signal-to-noise ratio (SNR). Furthermore, an incorrect estimate of the frame offset or phase ambiguity results in complete uncertainty about the information bits. Taking a hypothesis testing approach, the number of phase ambiguities that must be considered is well defined since this is determined by the modulation scheme. However, the number of frame offsets which must be considered is not obvious. In previous work on code-aided frame timing estimation, an assumption has been made regarding the uncertainty of the frame offset. For example, in [5] it is assumed that the number of possible frame offsets is fixed and simulations are performed assuming three possible offsets. In [7], it is assumed that the frame offset is known to be within a fixed window.

The results of [5] and [7] demonstrate that reliable frame timing estimation can be performed in an iterative receiver. However, due to the hypothesis testing approach, this comes at the cost of individually decoding each considered frame offset. Therefore, the cost of performing code-aided frame timing estimation is linearly dependent on the number of frame offsets which must be processed by the iterative receiver. The first contribution of this work is to characterize the frame offset distribution in order to evaluate the complexity of code-aided frame timing estimation. In a practical system, the receiver does not have prior knowledge of the values that the frame offset may take. Therefore, a method is provided for determining, on a frame-by-frame basis, *how many* and *which* frame offsets to process in the iterative receiver.

The second contribution of this work is to consider the design of an iterative receiver to perform joint estimation of the channel gain, carrier phase, symbol timing, frame timing, and noise power and detection of the information bits. The

[1]Knowledge of the data can come from pilot symbols or through feedback from the decoder when rotations by the phase ambiguity do not lead to valid codewords.

receiver performs the following functions: (a) non-data-aided coarse estimation of the continuous parameters (channel gain, phase offset, symbol timing, and noise power), (b) frame offset characterization to select the frame offsets processed by the iterative receiver, (c) hypothesis testing of the discrete parameters (phase ambiguity and frame offset), (d) EM-based fine estimation of the continuous parameters, and (e) posterior symbol and bit probability computation using the sum-product algorithm (SPA). In the numerical results, attention is given to the complexity of the iterative receiver.

II. System Model

We consider a system in which the information bits are encoded with an error-correction code and modulated with a digital phase-amplitude modulation to produce a symbol sequence $\mathbf{y} = [y_0, y_1, \ldots, y_{K-1}]$. Packets containing a single codeword (K symbols) are transmitted in bursts. Thus, synchronization must be performed on each packet. The channel introduces unknown attenuation α, carrier phase shift ϕ, delay τ, and additive white Gaussian noise. The received signal is expressed as

$$r(t) = \alpha e^{j\phi} \sum_{k=0}^{K-1} y_k p(t - kT - \tau) + w(t), \tag{1}$$

where $p(t)$ is a unit-energy pulse shape for which $g(t) = p(t) * p(-t)$ satisfies the Nyquist condition for zero intersymbol interference, T is the symbol period, and $w(t)$ is a complex Gaussian random process.

As explained in Section I, the phase offset is separated into an integer component ψ corresponding to a multiple of the phase ambiguity (that is, the phase by which a constellation can be rotated and maintain an identical form) and a continuous component χ such that $\phi = (\frac{2\pi}{\Psi}\psi + \chi)$. For phase shift keying (PSK) constellations, Ψ is equal to the modulation order and for quadrature amplitude modulation (QAM) constellations $\Psi = 4$. Furthermore, let the delay be separated into an integer multiple of the symbol period η and a fractional symbol period ϵ such that $\tau = (\eta + \epsilon)T$ where $-1/2 \leq \epsilon < 1/2$. Making these substitutions, the output of the matched filter is given by

$$\begin{aligned} x(t) &= r(t) * p(-t) \\ &= \alpha e^{j(\frac{2\pi}{\Psi}\psi + \chi)} \sum_{k=0}^{K-1} y_k g(t - (k + \eta + \epsilon)T) + n(t) \end{aligned} \tag{2}$$

where $n(t) = \int_{-\infty}^{\infty} w(a)p(a - t)da$ is filtered noise.

III. Frame Timing

The iterative receiver structure described in Section IV will take advantage of feedback from the decoder in order to perform reliable frame offset estimation. In this section, we consider the problem of choosing which frame offsets to process in the iterative receiver. We apply Bayesian techniques to obtain a posterior distribution on η which is used to decide on the number of frame offsets to consider. We then supply the iterative receiver with the highest probability offsets.

We introduce characterization of the frame offset distribution *assuming knowledge of the other parameters*. Furthermore, for the purpose of frame characterization, we assume that the symbols are independent and identically distributed (iid). Let the number of possible frame offsets be H such that $\eta \in (0, 1, \ldots, H-1)$. After matched filtering, samples taken at the (known) symbol offset are given by

$$\begin{aligned} x_l &= x((l + \epsilon)T) \\ &= \alpha e^{j(\frac{2\pi}{\Psi}\psi + \chi)} \sum_{k=0}^{K-1} y_k g((l - k - \eta)T) + n_l \\ &= \begin{cases} \alpha e^{j(\frac{2\pi}{\Psi}\psi + \chi)} y_{l-\eta} + n_l & l = \eta, \ldots, \eta + K - 1 \\ n_l & \text{otherwise} \end{cases}, \end{aligned} \tag{3}$$

where $n_l = n((l + \epsilon)T)$ are iid complex Gaussian random variables with variance σ^2. The sequence of samples is denoted $\mathbf{x} = [x_0, \ldots, x_l, \ldots, x_{L-1}]$ where $L = K + H - 1$. We assume that the number of offsets included in the sampling process H is large to ensure that the true offset has been included and to allow proper characterization of the frame offset's posterior distribution. For this reason, it is impractical (and unnecessary) to decode all H offsets.

The posterior distribution of the frame offset is expressed as

$$p(\eta|\mathbf{x}) \propto f(\mathbf{x}|\eta)p(\eta), \tag{4}$$

where, for the time being, all other parameters are assumed to be known and the symbols are assumed equally likely. The prior distribution for η is selected to be uniform over the domain of η. That is, $p(\eta) = \frac{1}{H}$ which, being a constant, may be dropped. Removing proportional constants and integrating out the phase ambiguity (due to the assumption of equally likely symbols), the posterior distribution of η is given by

$$\begin{aligned} &p(\eta|\mathbf{x}) \propto \\ &\prod_{k=0}^{K-1} \sum_{y_k \in \mathcal{Y}} \exp\left\{ \frac{1}{\sigma^2} \left(2\alpha \Re\left\{ e^{-j\chi} x_{k+\eta} y_k^* \right\} - \alpha^2 |y_k|^2 \right) \right\}, \end{aligned} \tag{5}$$

where $\mathcal{Y}$ is the set of all constellation points. To determine the probability of a particular offset, the posterior distribution is normalized so that it sums to one.

Given a subset of the H frame offsets, the probability that the true offset has been excluded from this subset is denoted P_{ex}. We desire to find the smallest subset of frame offsets which has a P_{ex} less than or equal to a specified value. This set is known as the highest posterior density (HPD) region which we will denote by $\mathcal{S}$ with size $|\mathcal{S}|$. For example, to limit the probability of exclusion to $P_{ex} = 0.01$, the set of frame offsets $\mathcal{S}$ which must be processed by the iterative receiver is given by the 99% HPD region. An example posterior distribution is shown in Fig. 1 where the 99% HPD is shown with marker "x". In this example, the HPD region contains seven offsets: $\{15, 22, 23, 24, 25, 26, 27\}$. The number of offsets is dynamically chosen when determining the HPD and, as seen in Fig. 1, need not be contiguous.

Since, α, χ, ϵ, and σ^2 are not known, we use non-data-aided estimates to characterize the frame offset distribution in the receiver. This is analogous to the Quasi Hybrid Likelihood Approach taken for detection and classification problems [8]. When simulating the iterative receiver's performance in Section V-B, we use this approach.

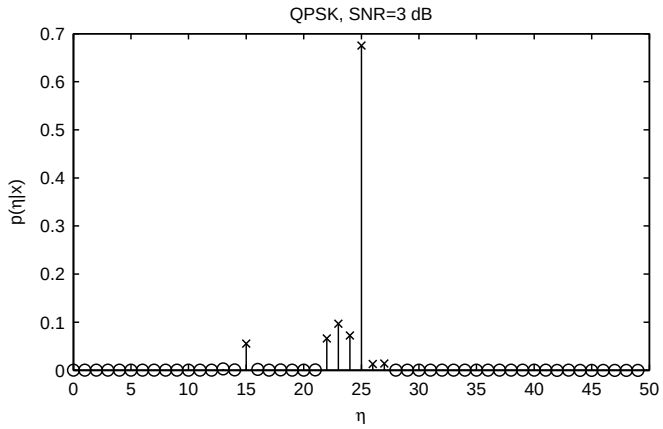

Fig. 1. Example posterior distribution and 99% highest posterior density region (shown with 'x') with true offset $\eta = 25$.

IV. Iterative Receiver Structure

The iterative receiver is based on the expectation maximization (EM) algorithm [9] which provides a means of estimating parameter $\boldsymbol{\theta}$ from incomplete data $\mathbf{r}$ when there exists a set of unobserved or missing data $\mathbf{y}$. Maximization is performed on the complete data $\mathbf{z} = [\mathbf{r}, \mathbf{y}]$ which typically simplifies computation. The benefit of the EM algorithm, in our application, is that it enables the receiver to work with marginal symbol probabilities rather than symbol sequence probabilities as would be required in a maximum likelihood receiver. The EM algorithm is given by the following expectation (E) and maximization (M) steps:

$$\text{E step: } Q(\boldsymbol{\theta}, \hat{\boldsymbol{\theta}}^{(p-1)}) = \int_{\mathbf{z}} f(\mathbf{z}|\mathbf{r}, \hat{\boldsymbol{\theta}}^{(p-1)}) \ln f(\mathbf{z}|\boldsymbol{\theta}) d\mathbf{z} \quad (6)$$

$$\text{M step: } \hat{\boldsymbol{\theta}}^{(p)} = \arg\max_{\boldsymbol{\theta}} Q(\boldsymbol{\theta}, \hat{\boldsymbol{\theta}}^{(p-1)}) \quad (7)$$

Since we are concerned with maximization, the E step can be simplified to [1]

$$Q(\boldsymbol{\theta}, \hat{\boldsymbol{\theta}}^{(p-1)}) = \sum_{\mathbf{y}} f(\mathbf{y}|\mathbf{r}, \hat{\boldsymbol{\theta}}^{(p-1)}) \ln f(\mathbf{r}|\mathbf{y}, \boldsymbol{\theta}). \quad (8)$$

In our case, let $\mathbf{r}$ represent the projection of $r(t)$ onto a complete orthonormal basis; let $\mathbf{y}$ be the transmitted symbol sequence; and define $\boldsymbol{\theta} = [\alpha, \chi, \epsilon, \sigma^2]$. In the expectation step, posterior probabilities of the symbols are obtained for the previous estimate $\boldsymbol{\theta}^{(p-1)}$ using the sum-product algorithm SPA operating on a factor graph of the demodulator and decoder. Since maximization over $\boldsymbol{\theta}$ is still complex, we make use of the expectation conditional maximization (ECM) algorithm [10]. The ECM algorithm is a variant of EM which involves sequentially performing maximization over each parameter while conditioning on the remaining parameters. Because parameters ψ and η are discrete, a hypothesis testing approach is taken as considered in [6]. The ECM algorithm is applied for each set $\{\tilde{\psi}, \tilde{\eta}\}$ where $\tilde{\psi} \in \{0, 1, \ldots, \Psi - 1\}$ and $\tilde{\eta} \in \mathcal{S}$.

The three components of the receiver: expectation, conditional maximization, and hypothesis testing are considered in the three sections which follow. To simplify the notation we define $\mathbf{x}_\eta(\epsilon) = [x_\eta(\epsilon), \ldots, x_{\eta+K-1}(\epsilon)]$ where $x_l(\epsilon) = x((l+\epsilon)T)$.

A. Expectation

The expectation step requires computing posterior probabilities $p\big(y_k \big| \mathbf{r}, \hat{\boldsymbol{\theta}}^{(p-1)}\big)$. From these probabilities, the expectations required for maximization in Section IV-B are

$$\bar{y}_k^{(p)} = \sum_{y_k \in \mathcal{Y}} y_k p\big(y_k \big| \mathbf{r}, \hat{\boldsymbol{\theta}}^{(p-1)}\big), \text{ and} \quad (9)$$

$$\bar{y^2}_k^{(p)} = \sum_{y_k \in \mathcal{Y}} |y_k|^2 p\big(y_k \big| \mathbf{r}, \hat{\boldsymbol{\theta}}^{(p-1)}\big). \quad (10)$$

The SPA and factor graphs provide a means of computing the posterior symbol probabilities. This step also provides posterior probabilities for the information bits which are necessary for detection. The factor graph receives as input symbol likelihoods which are calculated with respect to samples taken at the symbol timing estimate, i.e., $p\big(x_{k+\tilde{\eta}}(\hat{\epsilon}^{(p-1)}) \big| y_k, \hat{\boldsymbol{\theta}}^{(p-1)}\big)$. A thorough discussion of factor graph representations of modulation and coding is presented in [11].

B. Conditional maximization

We begin by developing the conditional maximization of α, χ, and ϵ. The log-likelihood function of these parameters is known to be equivalent to the following [12]:

$$\begin{aligned} &\ln f(\mathbf{r}|\mathbf{y}, \alpha, \chi, \epsilon) \propto \\ &-\int_{-\infty}^{\infty} \left| r(t) - \alpha e^{j\left(\frac{2\pi}{\Psi}\tilde{\psi} + \chi\right)} \sum_{k=0}^{K-1} y_k p(t - (k + \tilde{\eta} + \epsilon)T) \right|^2 dt \\ &\propto 2\alpha \Re\left\{ e^{-j\left(\frac{2\pi}{\Psi}\tilde{\psi} + \chi\right)} \sum_{k=0}^{K-1} y_k^* x_{k+\tilde{\eta}}(\epsilon) \right\} - \alpha^2 \sum_{k=0}^{K-1} |y_k|^2 \end{aligned} \quad (11)$$

Substituting (11) into the E step expression from (8) produces

$$\begin{aligned} &Q(\boldsymbol{\theta}, \hat{\boldsymbol{\theta}}^{(p-1)}) = \\ &2\alpha \Re\left\{ e^{-j\left(\frac{2\pi}{\Psi}\tilde{\psi} + \chi\right)} \sum_{k=0}^{K-1} \left(\bar{y}_k^{(p)}\right)^* x_{k+\tilde{\eta}}(\epsilon) \right\} - \alpha^2 \sum_{k=0}^{K-1} \bar{y^2}_k^{(p)}. \end{aligned} \quad (12)$$

The maximization step for ϵ is computed using a Newton-Raphson method as proposed by [3]. The pth update of ϵ is obtained from

$$\hat{\epsilon}^{(p)} = \hat{\epsilon}^{(p-1)} - \left. \frac{\left(\frac{\partial Q(\boldsymbol{\theta}, \hat{\boldsymbol{\theta}}^{(p-1)})}{\partial \epsilon}\right)}{\left(\frac{\partial^2 Q(\boldsymbol{\theta}, \hat{\boldsymbol{\theta}}^{(p-1)})}{\partial \epsilon^2}\right)} \right|_{\epsilon = \hat{\epsilon}^{(p-1)}} \quad (13)$$

Finite difference approximations to the first and second order partial derivatives are calculated by sampling the matched filtered signal at $t = (k + \hat{\epsilon}^{(p-1)} - \Delta)T$ and $t = (k + \hat{\epsilon}^{(p-1)} + \Delta)T$ where $0 < \Delta << 1$.

After obtaining $\hat{\epsilon}^{(p)}$, estimates of α and χ are calculated conditioned on the new symbol timing estimate. The parameters χ and α are updated during the same conditional maximization step because their updates do not depend on each

$$\ln f(\mathbf{x}_{\tilde{\eta}}(\hat{\epsilon}^{(p)})|\mathbf{y},\sigma^2) \propto -K\ln\pi\sigma^2 - \frac{1}{\sigma^2}\left(\sum_{k=0}^{K-1}|x_{k+\tilde{\eta}}(\hat{\epsilon}^{(p)})|^2 - 2\hat{\alpha}^{(p)}\Re\left\{e^{-j\left(\frac{2\pi}{\Psi}\tilde{\psi}+\hat{\chi}^{(p)}\right)}y_k^* x_{k+\tilde{\eta}}(\hat{\epsilon}^{(p)})\right\} + \hat{\alpha}^{(p)^2}|y_k|^2\right) \quad (14)$$

$$\hat{\sigma^2}^{(p)} = \frac{1}{K}\left(\sum_{k=0}^{K-1}|x_{k+\tilde{\eta}}(\hat{\epsilon}^{(p)})|^2 - 2\hat{\alpha}^{(p)}\Re\left\{e^{-j\left(\frac{2\pi}{\Psi}\tilde{\psi}+\hat{\chi}^{(p)}\right)}\left(\bar{y}_k^{(p)}\right)^* x_{k+\tilde{\eta}}(\hat{\epsilon}^{(p)})\right\} + \hat{\alpha}^{(p)^2}\bar{y^2}_k^{(p)}\right) \quad (15)$$

other. The estimates of α and χ which conditionally maximize $Q(\boldsymbol{\theta},\hat{\boldsymbol{\theta}}^{(p-1)})$ are

$$\hat{\alpha}^{(p)} = \frac{\left|\sum_{k=0}^{K-1}\left(\bar{y}_k^{(p)}\right)^* x_{k+\tilde{\eta}}(\hat{\epsilon}^{(p)})\right|}{\sum_{k=0}^{K-1}\bar{y^2}_k^{(p)}} \text{ and} \quad (16)$$

$$\hat{\chi}^{(p)} = \arg\left\{e^{-j\frac{2\pi}{\Psi}\tilde{\psi}}\sum_{k=0}^{K-1}\left(\bar{y}_k^{(p)}\right)^* x_{k+\tilde{\eta}}(\hat{\epsilon}^{(p)})\right\}, \quad (17)$$

respectively.

The noise power estimate is necessary to determine the symbol likelihoods used by the SPA as discussed in Section IV-A. Since the maximization of σ^2 is conditioned on ϵ, we use the log-likelihood function of the sampled matched filter output which is given in (14). Finally, the noise power update equation is given in (15).

C. Hypothesis testing

The authors of [6] present a code-aided hypothesis test which is analogous to the EM algorithm. Following their work, the E step requires evaluation of (12) for each hypothesis $\{\tilde{\psi},\tilde{\eta}\}$. In order to handle the continuous parameters $\boldsymbol{\theta}$, we apply a composite hypothesis test approach. For each hypothesis, after performing P iterations, estimates $\boldsymbol{\theta}^{(P)}$ and expectations $\bar{y}_k^{(P)}$ and $\bar{y^2}_k^{(P)}$ are used to evaluate (12). The hypothesis test is given by

$$[\hat{\psi},\hat{\eta}] = \arg\max_{\tilde{\psi},\tilde{\eta}} Q\left(\boldsymbol{\theta},\hat{\boldsymbol{\theta}}^{(P-1)}|\tilde{\psi},\tilde{\eta}\right)\Big|_{\boldsymbol{\theta}=\hat{\boldsymbol{\theta}}^{(P)}}, \quad (18)$$

where the dependence on $\{\tilde{\psi},\tilde{\eta}\}$ has been added.

V. Numerical Results

A. Frame timing

Results are first presented for the characterization of the HPD region of the frame offset. Simulations are presented in Figs. 2 and 3 for 16QAM and the assumption that all other synchronization parameters are known. In Fig. 2 the mean sizes of the 99% HPD, 99.9% HPD, and 99.99% HPD regions ($P_{ex} = 10^{-2}, 10^{-3}, 10^{-4}$, respectively) are presented. In Fig. 3 the P_{ex} achieved in simulation is shown for the three HPDs. The achieved P_{ex} is lower than the target value because an integer number of offsets must be chosen. The results demonstrate the effectiveness of the proposed approach to selecting frame offsets to process in the iterative receiver.

The best decision that a non-iterative receiver can make—assuming equally likely symbols—is to choose the frame offset that maximizes the likelihood, i.e., the ML offset. In contrast,

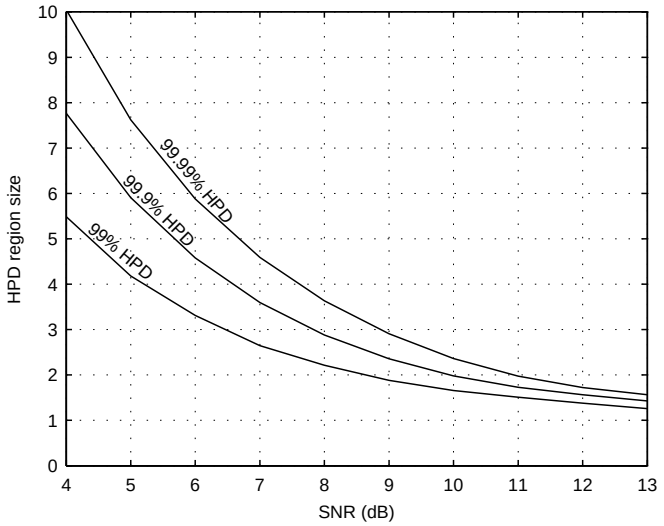

Fig. 2. Mean HPD region size with 16QAM modulation.

recall that the iterative receiver seeks to approximate the MAP solution to the *joint* detection and synchronization problem using feedback from the decoder. For comparison, Fig. 3 also shows the P_{ex} of the ML estimate (i.e., $Pr(\eta \neq \hat{\eta}_{\text{ML}})$) achieved by the non-iterative receiver. The main conclusion from this comparison is that, even for relatively high SNR, the P_{ex} of the HPD region is at least two orders of magnitude lower than that of the ML estimate.

Due to the hypothesis testing approach for frame offset detection in the iterative receiver, each frame offset must be demodulated and decoded. Thus, processing two offsets represents approximately a doubling of complexity versus processing a single offset. From Figs. 2 and 3, we can determine the complexity required for a given lower bound on performance. For $P_{ex} = 10^{-4}$ the mean HPD size is 8.1 at 4.8 dB (the Shannon bound for 2 bits/channel use) while at a moderate SNR of 8 dB the mean HPD size is 3.6.

B. Iterative Receiver Performance

The performance of the iterative receiver is evaluated for a transmission length of 1000 information bits, 16QAM modulation and a 1/2-rate turbo code ($K = 500$). The Oerder and Meyr (O&M) timing detector is used to obtain a coarse estimate of the symbol timing [13] and moment based estimates are obtained for α, χ, and σ^2 [8]. Energy detection is used to find the maximum energy frame offset of the received signal. Then the domain of the frame offset is set relative to this point. We found $H = 51$ to be sufficiently large to ensure that the true offset is always included in the frame offset characterization. In

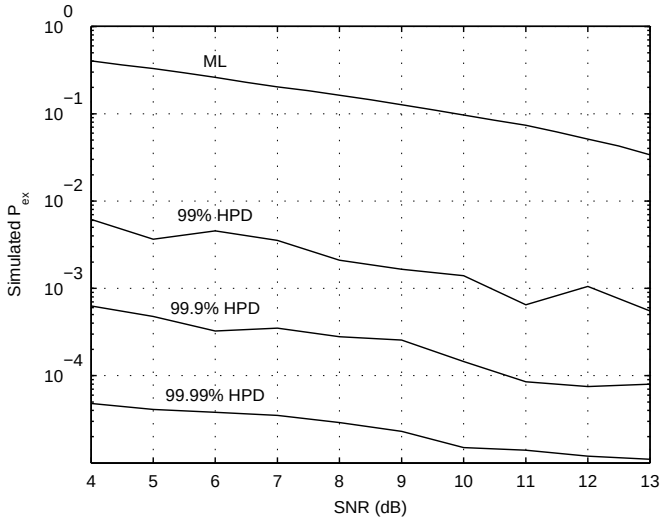

Fig. 3. P_{ex} of the HPD regions and of the ML estimate with 16QAM modulation.

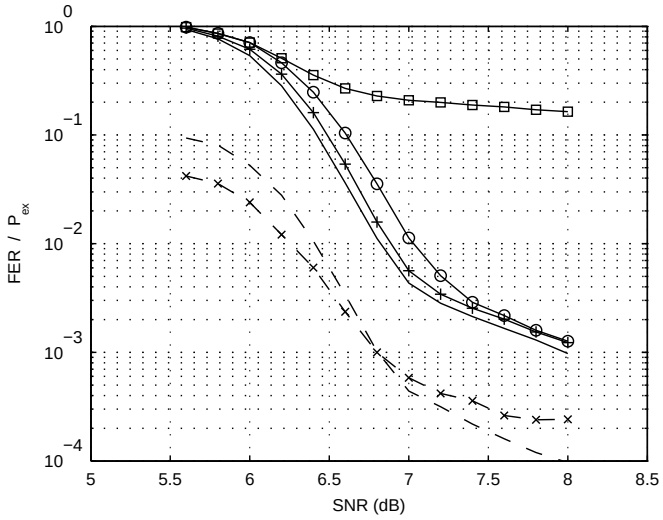

Fig. 4. Results for the FER for Perfect sync. (solid), HT (solid,circle), HT/ECM (solid,plus), and HT/ECM, ML frame offset (solid,square) as well as the target P_{ex} (dash) and the achieved P_{ex} (dash,'x').

order to minimize complexity without significant performance loss, the target P_{ex} was set to be $1/10$th of the codeword error rate with perfect synchronization. For each hypothesis, $P = 10$ iterations of the ECM algorithm are performed, each of which include a single iteration of the SPA[2].

Simulation results of the frame error rate (FER) are presented for four cases: (1) iterative demodulation and decoding with perfect synchronization (Perfect sync.); (2) hypothesis testing of ψ, η with no iterative estimation of the other parameters (HT); (3) the full iterative receiver with hypothesis testing and the ECM algorithm (HT/ECM); and (4) the full iterative receiver which only considers the ML estimate from the frame offset characterization stage (HT/ECM, ML frame offset). The performance of each case is shown in Fig 4. The iterative receiver demonstrates performance very near to that of perfect synchronization. In other words, the iterative receiver's ability to perform code-aided synchronization is on the same order as the decoder's ability to successfully decode the information in an ideal channel. Limiting the iterative receiver to only hypothesis testing results in a loss of 0.1-0.2 dB. The performance of the fourth case—considering only the ML frame offset estimate—quickly becomes limited by the P_{ex} (as observed in Fig. 3).

In the iterative receiver, the frame offset posterior distribution is characterized using the coarse estimates of α, χ, ϵ, and σ^2. In Fig. 4, the achieved P_{ex} for the iterative receiver performance simulation is shown. When the target P_{ex} is below 10^{-3}, we observe an increase in the probability of excluding the true frame offset from the HPD region as a result of errors in the coarse estimation stage, although the increase is slight.

Table I highlights the frame error performance of the receivers at SNR=7 dB. The number of frame errors is shown by receiver type. Frame errors may originate from excluding the true frame offset from $\mathcal{S}$, choosing an incorrect hypothesis when the true offset has been included in $\mathcal{S}$, and incorrect detection of one or more information bits when the true hypothesis has been chosen. The first two cases generally lead to half the bits being in error (i.e., the BER is significantly affected). The third case generally results in fewer bit errors.

During the frame offset characterization, the true offset was excluded from the HPD region in 30 simulations, which affects both the HT and HT/ECM receivers. When the true offset is included, the HT/ECM receiver always selected the correct hypothesis. Thus, the limiting factor is the frame characterization. We found that the improved estimates obtained by the ECM algorithm enables more reliable selection of the hypothesis.

In Fig. 5, the bit error rate (BER) performance of the receiver is shown. On the bit level, there is a significant difference in performance between perfect synchronization and the iterative receiver. This is primarily due to cases where the true offset was excluded from the HPD region. This is verified in Fig. 6 which shows only those simulations in which the true frame offset is included in $\mathcal{S}$. In Fig. 6, the BERs of perfect synchronization and HT/ECM are nearly identical while the BER of the HT receiver is higher because hypothesis errors are still made when the true offset is included. This agrees with the data presented in Table I. To achieve the BERs shown in Fig. 6, a larger HPD region is necessary, thereby increasing complexity.

TABLE I. NUMBER OF FRAME ERRORS ACCORDING TO THE SOURCE OF THE ERROR AT SNR=7 dB

Receiver Type	Total No. Frame Errors†	Exclusion	Inclusion	
		$\eta \notin \mathcal{S}$	Wrong Hypothesis	Noise
Perfect Sync.	200	0	0	200
HT	521	30	32	459
HT/ECM	254	30	0	224

†The total number of frames in the simulation is 47 683.

[2]Construction of the factor graph and SPA computations were performed using the Dimple probabilistic processing software [14].

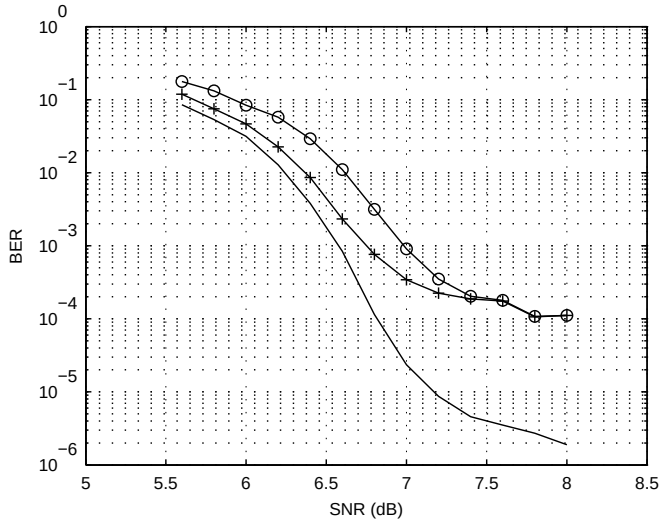

Fig. 5. BER of Perfect sync. (solid), HT (solid,circle), and HT/ECM (solid,plus) for all simulations.

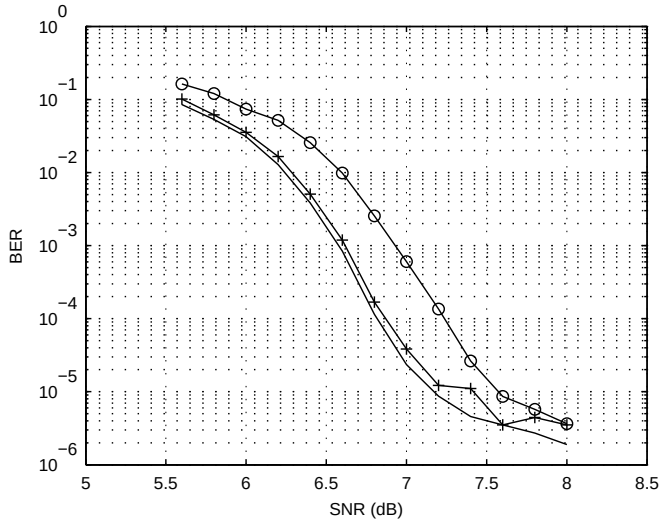

Fig. 6. BER of Perfect sync. (solid), HT (solid,circle), and HT/ECM (solid,plus) where we have excluded simulations in which the true offset is not in $\mathcal{S}$.

C. Iterative Receiver Complexity

The dominant source of complexity is from individually demodulating and decoding each hypothesis. The iterative receiver processes $\Psi \cdot |\mathcal{S}|$ hypotheses. Returning to the example from Section V-A with SNR = 8 dB, the average number of hypotheses is 14.4 ($\Psi = 4$, $|\mathcal{S}| = 3.6$). With $P = 10$, the iterative receiver requires a total of 144 decoder iterations on average in comparison to 10 for a traditional receiver (a factor of 14.4).

However, we found through simulation that after performing a single iteration of the ECM algorithm for each hypothesis, detection of the phase ambiguity and frame offset is reliable. After the hypothesis is chosen, further iterations of ECM are run to correctly detect the information bits. Thus, from our example, an iterative receiver would require an average of 14.4 iterations for hypothesis testing and 9 iterations to complete ECM algorithm for the selected hypothesis. A total of 23.4 decoder iterations are required on average, making the complexity of the iterative receiver $2.34\times$ that of the traditional receiver. The ECM algorithm does not significantly increase the complexity of the receiver because it is embedded into the decoding process [1].

VI. Conclusion

In this paper, an iterative receiver capable of performing synchronization without the use of a preamble was presented. The structure, performance, and complexity of the receiver was considered with specific attention given to frame timing synchronization. A method based on the highest posterior density region was proposed for determining how many and which frame offsets to process in the iterative receiver. This method provides control over the complexity and performance of the receiver. The results demonstrate that the iterative receiver achieves a FER near to that of perfect synchronization with reasonable complexity in comparison to a traditional receiver aided by a preamble.

References

[1] N. Noels, C. Herzet, A. Dejonghe, V. Lottici, H. Steendam, M. Moeneclaey, M. Luise, and L. Vandendorpe, "Turbo synchronization: an EM algorithm interpretation," in *Proc. 2003 IEEE Int. Conf. Communications (ICC)*, vol. 4, pp. 2933–2937.

[2] N. Noels, V. Lottici, A. Dejonghe, H. Steendam, M. Moeneclaey, M. Luise, and L. Vandendorpe, "A theoretical framework for soft-information-based synchronization in iterative (turbo) receivers," *EURASIP J. Wireless Commun. Netw.*, vol. 2005, no. 2, pp. 117–129, Apr. 2005.

[3] C. Herzet, V. Ramon, L. Vandendorpe, and M. Moeneclaey, "EM algorithm-based timing synchronization in turbo receivers," in *Proc. 2003 IEEE Int. Conf. Acoustics, Speech, and Signal Processing (ICASSP)*, vol. 4, pp. IV–612–IV–615.

[4] C. Herzet, H. Wymeersch, M. Moeneclaey, and L. Vandendorpe, "On maximum-likelihood timing synchronization," *IEEE Trans. Commun.*, vol. 55, no. 6, pp. 1116–1119, June 2007.

[5] H. Wymeersch, H. Steendam, H. Bruneel, and M. Moeneclaey, "Code-aided frame synchronization and phase ambiguity resolution," *IEEE Trans. Signal Process.*, vol. 54, no. 7, pp. 2747–2757, July 2006.

[6] C. Herzet, H. Wymeersch, F. Simoens, M. Moeneclaey, and L. Vandendorpe, "MAP-based code-aided hypothesis testing," *IEEE Trans. Wireless Commun.*, vol. 7, no. 8, pp. 2856–2860, Aug. 2008.

[7] J. Sun and M. Valenti, "Optimum frame synchronization for preambleless packet transmission of turbo codes," in *Conf. Rec. Thirty-Eighth Asilomar Conf. Signals, Systems and Computers*, 2004, pp. 1126–1130.

[8] A. Abdi, O. Dobre, R. Choudhry, Y. Bar-ness, and W. Su, "Modulation classification in fading channels using antenna arrays," in *Proc. 2004 IEEE Military Communications Conf. (MILCOM)*, vol. 1, pp. 211–217.

[9] A. P. Dempster, N. M. Laird, and D. B. Rubin, "Maximum likelihood from incomplete data via the EM algorithm," *J. Roy. Stat. Soc., Ser. B*, vol. 39, no. 1, pp. 1–38, Jan. 1977.

[10] X. L. Meng and D. B. Rubin, "Maximum likelihood estimation via the ECM algorithm: A general framework," *Biometrika*, vol. 80, no. 2, pp. 267–278, Jun. 1993.

[11] H. Wymeersch, *Iterative Receiver Design*. Cambridge Univ. Press, 2007.

[12] U. Mengali and A. N. D'Andrea, *Synchronization techniques for digital receivers*. New York: Plenum Press, 1997.

[13] M. Oerder and H. Meyr, "Digital filter and square timing recovery," *IEEE Trans. Commun.*, vol. 36, no. 5, pp. 605–612, May 1988.

[14] S. Hershey, J. Bernstein, B. Bradley, A. Schweitzer, N. Stein, T. Weber, and B. Vigoda, "Accelerating inference: towards a full language, compiler and hardware stack," *arXiv:1212.2991*, Dec. 2012.